Suppression of Protein Structure Destabilizing Mutations in *Bacillus thuringiensis* δ-Endotoxins by Second Site Mutations†

Brian D. Almond* and Donald H. Dean

Departments of Molecular Genetics and Biochemistry, The Ohio State University, Columbus, Ohio 43210

Received July 10, 1992; Revised Manuscript Received September 30, 1992

ABSTRACT: Reciprocal exchange of a small region (residues 428–450) within the specificity determining region of two *Bacillus thuringiensis* δ-endotoxins, CryIAa and CryIAc, resulted in two recombinant proteins that possess a decreased insecticidal activity to *Bombyx mori* and *Manduca sexta*. Site-directed mutations introduced in this region of one of the recombinant proteins, with the intent of restoring insecticidal activity, resulted in further reduction of toxicity. We determined that the loss of insecticidal activity in the mutants and the original recombinants was associated with altered toxin protein structure, as measured by sensitivity to intracellular and exogenous proteases. The structural instability of the site-directed mutant proteins could be suppressed genetically by subcloning the mutated region into *cryIAc* or by introducing second site mutations in defined regions of the mutated *cryIAa* gene. The second site mutations, by themselves, also produced unstable proteins. In the course of this study, we demonstrated that this small region does not suffice as a specificity determining region for *M. sexta*.

The bacterium *Bacillus thuringiensis* is a Gram-positive organism that produces a proteinaceous crystal insecticide during sporulation. The life cycle of the bacterium starts when the spore and crystal insecticide are ingested by a susceptible insect. The crystal is solubilized in the high pH and reducing environment of the insect midgut and dissolves into 130 000-Da[1] protoxin subunits. The protoxin is digested by trypsin-like proteases within the insect midgut to form a 65 000-Da active toxin (Huber et al., 1981). The toxin is stable to further trypsin digestion and is referred to as the tryptic-resistant core (Chestukhina et al., 1982). The activated toxin is theorized to bind to specific insect midgut receptors located on the brush border membrane of the columnar epithelial cells (Hofmann et al., 1988). The toxin creates a potassium ion (K^+) specific pore which allows influx of potassium ion into the epithelial cells, disrupting the membrane potential difference and allowing the influx of water. The influx of water causes the columnar epithelial cells to swell and lyse (Harvey & Wolfersberger, 1979). Disruption of the insect midgut epithelial cells results in paralysis of the insect and soon death results. The *B. thuringiensis* spores germinate and grow in the dead insect (Andrew et al., 1987).

A multitude of insecticidal crystal proteins have been isolated and identified; Höfte and Whiteley (1989) have categorized them by DNA sequence homology and insect specificity. The CryIA group consists of three members all active against *Lepidoptera*. The three members of this class, CryIAa, CryIAb, and CryIAc, share over 80% amino acid homology. Despite the close homology of the CryIA proteins, they differ considerably in insecticidal activity. CryIAa possess 400-fold more *Bombyx mori* (silkworm) bioassay activity than CryIAc (Ge et al., 1989). CryIAc, on the other hand, possess a 9-fold greater *Heliothis virescens* (tobacco budworm) and a 12-fold greater *Trichoplusia ni* (cabbage looper) bioassay activity than CryIAa (Ge et al., 1991). CryIAa and CryIAc demonstrate equal *Manduca sexta* (tobacco hornworm) bioassay activities (Milne et al., 1990).

Reciprocal exchanges of genetic material between the *cryIAa* and *cryIAc* genes were constructed by Ge et al. (1989, 1991) to localize specificity determining regions for various insects. The specificity determining region for *B. mori* on CryIAa is located within residues 332–450 (Ge et al., 1989). CryIAc regions 332–450 and 450–612 are theorized to be the *T. ni* and *H. virescens* specificity determining regions, respectively (Ge et al., 1991). An interesting pair of chimeric toxins used in this work is P4111 and P4211. P4111 is a chimeric protein consisting of CryIAa with residues 428–450 from CryIAc; P4211 is the reciprocal of P4111 with CryIAc residues 428–450 from CryIAa. Residues 428–450 are also referred to as the *Cla*I to *Sac*I region. In *B. mori* bioassays, P4111 has a 100-fold reduction in the LD_{50} value when compared to P4102 (CryIAa). P4211, also, demonstrated a large decrease in *B. mori* insecticidal activity when compared to P4202 (CryIAc), a decrease of at least 17-fold (Lee et al., 1991). In *H. virescens* bioassays, P4111 demonstrated at least a 2.2-fold decrease in toxicity and P4211 was shown to have a similar reduction in activity of 2.6-fold (Ge et al., 1990). The reduction in the *H. virescens* activity of both chimeric proteins is interesting in that the *H. virescens* specificity determining region is located outside of the *Cla*I–*Sac*I region of the CryIAc toxin. In theory, these residues in the *Cla*I–*Sac*I region are not directly involved in the *H. virescens* specificity determining region of the CryIAc toxin. In the *T. ni* bioassay, decreases in activity for P4111 and P4211 can also be found. P4111 and P4211 were shown to be stable to exogenous protease treatment and to generate 65 000-Da toxin when digested with trypsin (Ge et al., 1991), suggesting that no large protein structural alterations are present.

In a paper by Schnepf et al. (1990), a series of chimeric toxins was constructed by replacement of CryIAc residues with CryIAa residues. One of these chimeric proteins demonstrated a large reduction in *Manduca sexta* insecticidal activity. This chimeric toxin CC2 (CryIAc:CryIAa 429–447

† This work was supported by grants from the National Institutes of Health, AI29092, and the USDA Forest Service, Northeastern Forest Experiment Station.

* To whom correspondence should be addressed.

[1] Abbreviations: CryIA, δ-endotoxin protein; *cryIA*, δ-endotoxin gene; Da, daltons; pOS4102, plasmid pKK223-3 bearing a cloned δ-endotoxin gene; P4102, the protein expressed by the plasmid pOS4102; LD_{50}, lethal dose that results in 50% mortality; LC_{50}, lethal concentration that results in 50% mortality; Δ, a deletion; $EcoRI_2$, term used to represent the second *Eco*RI site present in the *cryIAa* gene.

0006-2960/93/0432-1040$04.00/0

residues replaced) is similar to construct P4211 (Ge et al., 1989). Because of this large reduction in *M. sexta* bioassay activity, the residues in region 429–447 are theorized to be the *M. sexta* specificity determining region.

The current paper attempts to elucidate the role the *Cla*I–*Sac*I region (nucleotides 1284–1350 corresponding to residues 428–450) plays in determining bioassay activity. Site-directed mutations were created within this *Cla*I–*Sac*I region to determine a possible role for the residues located within this region. *B. mori* and *M. sexta* bioassays were performed to determine the effect the mutagenesis has on the activity. Stability studies were used to ascertain the effect of the mutagenesis on the protein structure. We found that chimeric toxins involving this region or site-directed mutants created within this *Cla*I–*Sac*I region create detectable protein structural alterations. These alterations in protein structure were found to affect the bioassay activity. We observed that second site mutations could compensate for these structure altering mutations.

MATERIALS AND METHODS

General Molecular Biology Techniques. Site-directed mutagenesis was performed by the single oligonucleotide method with Kunkel selection (Kunkel, 1985). Single-stranded DNA phage were produced by use of helper phage M13KO7 and kanamycin selection (Vieira & Messing, 1982) for both site-directed mutagenesis and sequencing. Potential mutants were screened by the dideoxy sequencing method by use of Sequenase kit (U.S. Biochemicals). Bacterial stains used for this work include MV1190 [Δ*lac–proAB*, *thi*, *supE*, Δ(*srl–recA*)306::Tn10 (*tet*^{r}), F′:traD36, *proAB*, *lacI*^{q},*Z*Δ-*M153*] for site-directed mutagenesis and cloning and CJ236 (*dut*, *ung*, *thi*, *relA*, *pCJ105*) was used for production of single-stranded uracil-containing DNA templates for the Kunkel selection method.

Construction of Chimerical Toxins. The *Eco*RI$_2$–*Sac*I (nucleotides 996–1350 corresponding to residues 332–450) region of the construct pOS4111 (Ge et al., 1889) was cloned into the *Eco*RI–*Sac*I sites of the multiple cloning site of the vector pUC118. The resulting subclone is referred to as pBDA7. The subcloned region consisted of *Eco*RI–*Cla*I of *cryIAa* and *Cla*I–*Sac*I from *cryIAc*. Site-directed mutagenesis was performed on single-stranded uracil-containing DNA templates of pBDA7 with the assistance of five oligonucleotides. Oligonucleotide 1 (5′-AAAGCCTGAACGCATTGAAACATGGCT-3′) caused a loop-out deletion of bases 1305–1308 of the *cryIAc* section of pBDA7 which removed F_{435}, creating pBDA7/ΔF_{435}. Oligonucleotide 2 (5′-AAAGCCTGAAAGAAACATTGA-3′) altered bases 1308–1311 in the *cryIAc* section of pBDA7 creating pBDA7/R_{436}L. Oligonucleotide 3 (5′-ACTATTACTAAATTGTGGAACGAAACAT-3′) altered bases 1314–1317 in the *cryIAc* section of pBDA7, creating pBDA7/G_{438}Q. Oligonucleotide 4 (5′-CACTACTATTACTGCCTGAACGAAAC-3′) caused a loop-out deletion of bases 1317–1320 in pBDA7 which removed F_{439}, creating pBDA7/ΔF_{349}. Oligonucleotide 5 (5′-AGCTCTTATTATGTATACACTACTATT-3′) altered bases 1338–1341 in the *cryIAc* section of pBDA7 creating pBDA7/S_{446}Y. All potential mutants were sequenced by the Sequenase dideoxy DNA sequencing method (U.S. Biochemicals).

pOS4111/ΔF_{435}, pOS4111/R_{436}L, pOS4111/G_{438}Q, pOS-4111/ΔF_{439}, and pOS4111/S_{446}Y constructions were accomplished by digestion of pBDA7/site-directed mutants with *Eco*RI and *Sac*I and band isolation of the resulting 353-bp fragments. The *Eco*RI–*Sac*I fragments were then subcloned into pOS4102, i.e., *cryIAa* in bacterial protein overexpression plasmid pKK223-3 (Ge et al., 1989). The resulting constructs were referred to as pOS4111/site-directed mutants.

pOS4202/site-directed mutants were constructed by cloning the 280-bp *Eco*RI–*Cla*I fragment from pOS4202 (Ge et al., 1989) into *Eco*RI–*Cla*I-digested pBDA7/ΔF_{435}, pBDA7/R_{436}L, pBDA7/G_{438}Q, pBDA7/ΔF_{439}, and pBDA7/S_{446}Y, replacing the *cryIAa* section of pBDA7 mutants with *cryIAc*, also digested with *Eco*RI and *Cla*I. The resulting vectors were termed pBDA7/site-direct/pOS4202. The pBDA7/site-direct/pOS4202 constructs were then digested with *Eco*RI and *Sac*I and subcloned into pOS4202 also digested with *Eco*RI and *Sac*I. The resulting plasmids are termed pOS4202/ΔF_{435}, pOS4202/R_{436}L, pOS4202/G_{438}Q, pOS4202/ΔF_{439}, and pOS4202/S_{446}Y.

pOS4110 [i.e., *cryIAa* with nucleotides 996–1330 corresponding to residues 332–450 replaced with *cryIAc* (Ge et al., 1989)]/site-directed mutations were created by digestion of pBDA7/site-direct/pOS4202 with *Eco*RI and *Sac*I. After fragment isolation, the fragments were subcloned into pOS4102. The resulting constructs were named pOS4110/ΔF_{435}, pOS4110/R_{436}L, pOS4110/G_{438}Q, pOS4110/ΔF_{439}, and pOS4110/S_{446}Y.

Construction of the last chimerical toxin created for this work was done by addition of the *Sac*I–*Hin*dIII fragment from pOS4202 into the *Sac*I–*Hin*dIII sites in the multiple cloning region of the pBDA7/site-direct mutants. The resulting vector consisted of *Eco*RI–*Cla*I of *cryIAa* and *Cla*I–*Hin*dIII from *cryIAc*. This vector was digested with *Eco*RI and *Hin*dIII and cloned into the same sites in pOS4102. The resutling construct was named pBDA4123/ΔF_{435}, pBDA4123/R_{436}L, pBDA4123/G_{438}Q, pBDA4123/ΔF_{439}, or pBDA4123/S_{446}Y and consisted of *Cla*I–*Hin*dIII from *cryIAc* and *Eco*RI–*Cla*I from *cryIAa*.

Site-directed mutagenesis was performed in the form of blocks on pOS4111/G_{438}Q and pOS4111/S_{446}Y to localize compensation mutants for these two toxins. Block mutations changed pOS4111 *cryIAa* residues into their corresponding *cryIAc* residues. Block 2 consists of residues 347–349 (P_{347}Q, V_{348}Q, and L_{349}R). Residues 370–373 and residue 375 (I_{370}P, L_{371}F, G_{372}N, S_{373}I, P_{373}I, and P_{375}I) constituted block 3.

Crystal Purification and Protoxin Solubilization. The cells containing the mutant protoxins were grown in 2× YT media containing 50 μg/mL ampicillin for 72 h at 37 °C. To purify the crystals, the cells were pelleted and resuspended in 50 mL of lysing solution (15% sucrose, 50 mM EDTA, 50 mM Tris (pH 8.0) and 10 μg/mL lysozyme). The cells were incubated in lysing solution for 1 h at 37 °C and finally overnight at 4 °C. The cells were sonicated, and centrifuged, and the resulting pellet was washed three times with 0.5 M NaCl/2% Triton X-100, six times with 0.5 M NaCl, and finally once with deionized water. The crystals were solubilized in 50 mM Tris (pH 9.5) and 10 mM DTT for 2 h at 37 °C. After solubilization, the concentration of the protoxin was determined by the Coomassie protein determination kit (Pierce).

Bioassays. B. mori eggs were received from Ross Milne (Forestry Pest Management Institute, Sault Ste. Marie, Ontario, Canada). After hatching, they were raised on an exclusive diet of Mulberry leaves. *M. sexta* eggs were received from Michael Jackson (USDA Southern Cotton Research Laboratory, NC). Bioassays were performed essentially as described by McLinden et al. (1985). In *B. mori* bioassays, 25 μL of the diluted protoxins was added to a Mulberry leaf disc (1.5 cm in diameter). In the *M. sexta* bioassay, 25 μL of the protoxin diluted into 50 mM Tris (pH 9.5) was added to an artificial diet disc 1.5 cm in diameter. *B. mori* first

instar and *M. sexta* neonate larva were used for the bioassays. The larvae were placed on the diet in a container and incubated at room temperature. *B. mori* mortalities were recorded after 24 h, while *M. sexta* mortalities were recorded after 5 days. Twenty larvae were used for each of five protoxin concentrations. The bioassays were repeated five times for each insect species. The LC_{50} values and 95% confidence intervals were calculated according to the PROBIT method of Raymond (1985).

Determination of Altered Protein Structure. To determine if mutagenized protoxins were sensitive to intracellular *Escherichia coli* proteases, *E. coli* strain MV1190 containing the mutagenized genes was grown for 24 h at 37 °C in 2× YT media containing 50 μg/mL ampicillin. The cultures were concentrated to OD_{600} = 10.0, centrifuged, resuspended, and lysed in 200 μL of SDS–PAGE loading dye by boiling for 10 min. The insoluble material was pelleted by centrifugation; the soluble fraction was examined by SDS–PAGE (Laemmli, 1970). After the gel has been stained and destained, the 130 000-Da protoxin band is clearly visible above the *E. coli* bands.

To determine if any alterations in protein structure had occurred in the mutant toxins, protease digestion methods were employed. Trypsin digestion was used to determine if the mutant protoxins could form trypsin-resistant cores. One percent (w/w) trypsin was added to the protoxin solution and the solution was incubated 37 °C. After 1 h of incubation, another 1% (w/w) trypsin was added and incubation was continued for another hour at 37 °C. SDS–PAGE was used to monitor the transition from the 130 000-Da protoxin to the 65 000-Da toxin.

Thermolysin digestion was used to further analyze structural alterations of trypsin-resistant mutant toxins; the procedure employed was a modification of Gent et al. (1987). The conditions used for this work were optimized through experimentation. Toxin (300 μg) is incubated at various temperatures with 2% (w/w) thermolysin in 50 mM Tris (pH 9.5) and 10 mM $CaCl_2$ (final concentration). Aliquots that were calculated to contain 30 μg of toxin were withdrawn after 30 min of incubation at 37 °C, 43.5 °C, 50 °C, 52.5 °C, 55 °C, 57.5 °C, 60 °C, 62.5 °C, 65 °C, and 70 °C in a Brinkmann RM6 water bath. The digestion was terminated by addition of 20 mM EDTA (final concentration). Samples were analyzed by SDS–PAGE and Coomassie Brilliant Blue staining. To determine the relative amount of toxin remaining after thermolysin digestion at the indicated temperature, the band intensities were scanned with a densitometer (Hoefer, Inc.) and the area of the peaks was determined with a digitizer (Numonics, Inc.). The data were recorded as the percentage of the toxin remaining versus temperature. Linear regression was used to calculate a Ts value. The Ts value is the temperature at which 50% of the toxin remains.

RESULTS

Bioassay of Site-Directed Mutant Proteins on B. mori and M. sexta. Five site-directed mutations, ΔF_{435}, $R_{436}L$, $G_{438}Q$, ΔF_{439}, and $S_{446}Y$, were constructed in the chimerical gene pOS4111 (Figure 1). The mutant protoxins were analyzed by *B. mori* bioassay (Table I). The control P4102 (CryIAa protoxin) LC_{50} values were similar to those in published reports (Ge et al., 1989; Milne et al., 1990). P4111 shows a 6-fold reduction in *B. mori* toxicity when compared to P4102. When the mutant protoxins are compared to P4111, P4111/ΔF_{435} and P4111/$R_{436}L$ show a reduction of 1.5-fold and 1.9-fold in *B. mori* toxicity, respectivity. The other three mutant protoxins, P4111/$G_{438}Q$, P4111/ΔF_{439}, and P4111/$S_{446}Y$, demonstrated a greater than 2.3-fold decrease in *B. mori* toxicity relative to P4111.

	CryIAa		CryIAc	Mutations
ClaI (428)→				
	Arg		Arg	
	Leu		Leu	
	Ser		Ser	
	His		His	
	Val		Val	
	Thr	**	Ser	
	Met		Met	
	---	****	Phe	ΔF435
	Leu	****	Arg	R436L
	Ser		Ser	
	Gln	****	Gly	G438Q
	Ala	****	Phe	ΔF439
	Ala	**	Ser	
	Gly	****	Asn	
	Ala	**	Ser	
	Val	****	Ser	
	Tyr	****	Val	
	Thr	****	Ser	S446Y
	Leu	**	Ile	
	---	****	Ile	
	Arg		Arg	
	Ala		Ala	
SacI (450) →				

FIGURE 1: *cryIAa* vs *cryIAc* comparison within the *Cla*I–*Sac*I region (residues 428–450). The five site-directed mutations: ΔF_{435}, $R_{436}L$, $G_{438}Q$, ΔF_{439}, and $S_{446}Y$. Symbols: **, Dayhoff conserved group change; ****, Dayhoff nonconserved group change (21).

Table I: *Bombyx mori* Bioassay Data[a]

protoxin	LC_{50}	protoxin	LC_{50}
P4102	104.1 (80–134)[b]	P4111/$G_{438}Q$	>1500
P4111	643 (510–839)	P4111/ΔF_{439}	>1500
P4111/ΔF_{435}	985.8 (758–1351)	P4111/$S_{446}Y$	>1500
P4111/$R_{436}L$	1202.7 (966–1637)		

[a] Mulberry leaf discs were used in *B. mori* bioassays. LC_{50} represents total nanograms of protoxin added to the leaf disc. [b] 95% confidence range.

Table II: *Manduca sexta* Bioassay Data

protoxin	LC_{50}[a]	protoxin	LC_{50}[a]
P4102	9 (7–13)[b]	P4111/$R_{436}L$	36 (28–47)
P4202	12 (10–16)	P4111/$G_{438}Q$	>600
P4111	27 (22–36)	P4111/ΔF_{439}	>600
P4211	>600	P4111/$S_{446}Y$	>600
P4111/ΔF_{435}	38 (30–50)		

[a] LC_{50} is total nanograms of protoxin added to the artificial diet. [b] 95% confidence range.

Table II contains the results of the *M. sexta* bioassay. P4102 and P4202 demonstrate insecticidal activity in the range of published results (Schnepf et al., 1990; Milne et al., 1990). P4111 possesses close to a three-fold reduction in activity. P4211, which is the reciprocal construction of P4111, also shows a large decrease in toxicity, of at least 50-fold. The P4111/site-direct mutations all show decreases in *M. sexta* activity when compared to P4111. P4111/ΔF_{435} and P4111/$R_{436}L$ demonstrate a 1.4-fold and 1.3-fold reduction, respectfully. The last three P4111/site-direct mutations, P4111/$G_{438}Q$, P4111/ΔF_{439}, and P4111/$S_{446}Y$, possess at least a 22-fold reduction in *M. sexta* insecticidal activity.

Trypsin Digestion of P4111/Site-Directed Mutations. P4111/ΔF_{435} and P4111/$R_{436}L$, upon trypsin digestion, generate tryptic resistant cores similar to those of P4102 and

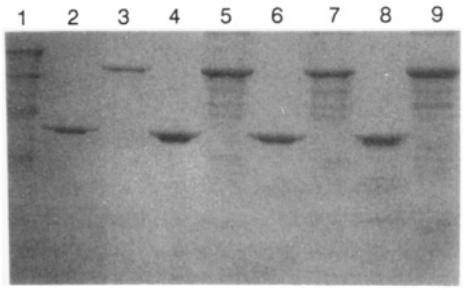

FIGURE 2: Trypsin digestion of P4102, P4111, P4111/ΔF_{435}, and P4111/R_{436}L. Lane 1, high molecular mass marker (200 kDa, 116.5 kDa, 80 kDa, and 49.5 kDa); lanes 2 and 3, P4102; lanes 4 and 5, P4111; lane 6 and 7, P4111/ΔF_{435}; lanes 8 and 9, P4111/R_{436}L. Trypsin digestion was in lanes 2, 4, 6, and 8.

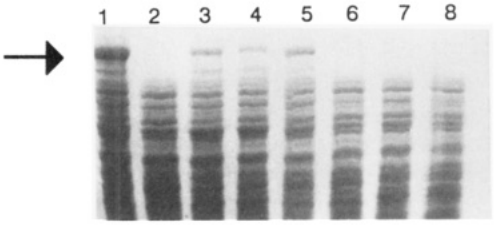

FIGURE 3: Twenty-four-hour whole cell lysates of pOS4111/site-direct mutants. Lane 1, pOS4102; lane 2, pKK223-3; lane 3, pOS4111; lane 4, pOS4111/ΔF_{435}, lane 5, pOS4111/R_{436}L; lane 6, pOS4111/G_{438}Q; lane 7, pOS4111/ΔF_{439}; lane 8, pOS4111/S_{446}Y. The arrow indicates the 130 000-Da protoxin band.

Table III: Temperature Midpoint for Thermolysin Sensitivity

toxin	Ts[a] mean	toxin	Ts[a] mean
P4102	61 ± 1	P4211	61 ± 1
P4202	67 ± 2	P4111/ΔF_{435}	56 ± 1
P4111	58 ± 1	P4111/R_{436}L	59 ± 1

[a] Ts values are in degrees Celsius. [b] Standard deviation in degrees Celsius.

P4111 (Figure 2). Mutations P4111/G_{438}Q, P4111/ΔF_{439}, and P4111/S_{446}Y do not generate 130 000-Da protoxin. To determine whether or not protoxin is being produced in these three mutants, whole cell lysates were analyzed by 7.5% SDS–PAGE. Figure 3 demonstrates that these three are highly sensitive to *E. coli* intracellular proteases by the absences of the protoxin band.

Protein Stability of P4111/ΔF_{435} and P4111/R_{436}L. The thermolysin/temperature procedure was used on the two P4111/site-direct mutants that produce tryptic-resistant cores. In Table III, P4111 can be seen to have a Ts value 3 °C lower than that of P4102. The data show that P4111/ΔF_{435} possess a 2 °C lower Ts value than P4111. On the other hand, P4111/R_{436}L demonstrates a 1 °C higher Ts value than that of P4111.

Suppression of Structural Instability. P4111/G_{438}Q, P4111/ΔF_{439}, and P4111/S_{446}Y mutants were shown to be sensitive to trypsin. When these three site-direct mutants were introduced into pOS4202 (an entire *cryIAc* background), an intact 130 000-Da protoxin could be isolated from each of the mutants. Furthermore, trypsin digestion of the P4202/site-directed mutants produces 65 000-Da trypsin-resistant toxic cores (Figure 4). In order to localize the region that allowed this structural compensation, two other switches involving subsets of *cryIAc* were constructed, pBDA4123 (nucleotides 1350–1704 corresponding to CryIAc residues 450–612) and pOS4110 (nucleotides 996–1284 corresponding to CryIAc residues 332–428). The data showed that trypsin-resistant cores did not form when PBDA4123/G_{438}Q or PBDA4123/S_{446}Y was digested with trypsin. Interestingly,

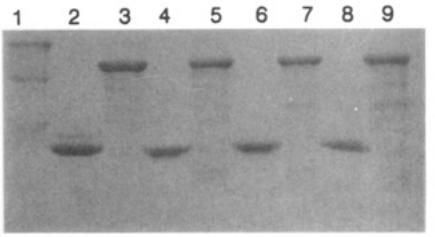

FIGURE 4: Trypsin digestion of P4202/site-direct mutants. Lane 1, high molecular mass marker mix (200 kDa, 116.25 kDa, and 80 kDa); lanes 2 and 3, P4202; lanes 4 and 5, P4202/G_{438}Q; lanes 6 and 7, P4202/ΔF_{439}; lanes 8 and 9, P4202/S_{446}Y. Lanes 2, 4, 6, and 8 are trypsin-digested samples.

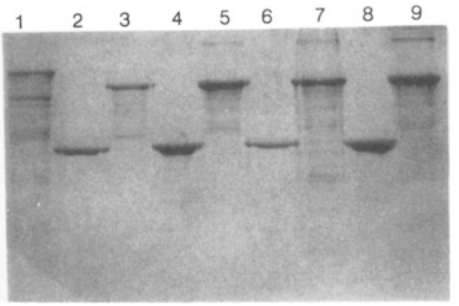

FIGURE 5: Trypsin digestion of P4110/site-direct mutants. Lane 1, high molecular mass marker (200 kDa, 116.25 kDa, 80 kDa, and 49.5 kDa); lanes 2 and 3, P4110; lanes 4 and 5, P4110/G_{438}Q; lanes 6 and 7, P4110/ΔF_{439}; lanes 8 and 9, P4110/S_{446}Y. Lanes 2, 4, 6, and 8 are digested with trypsin.

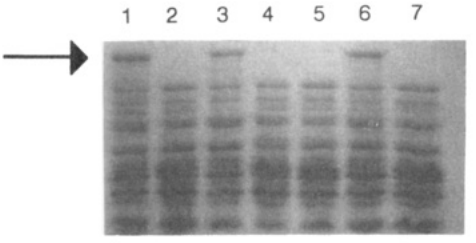

FIGURE 6: Twenty-four-hour whole cell lysates of block mutants. Lane 1, pOS4102; lane 2, pOS4111/G_{438}Q; lane 3, pOS4111/G_{438}Q/block 2; lane 4, pOS4111/G_{438}Q/block 3; lane 5, pOS4111/S_{446}Y; lane 6, pOS4111/S_{446}Y/block 2; lane 7, pOS4111/S_{446}Y/block 3. The arrow indicates the 130 000-Da protoxin band.

the protoxin proteins that were isolated (as in the case of PBDA4123/G_{438}Q) possessed a size less than 130 000 Da (data not shown). On the other hand, P4110 chimeric proteins did compensate for G_{438}Q, ΔF_{439}, and S_{446}Y as evidenced by the generation of tryptic-resistant cores (Figure 5, lanes 4, 6, and 8).

Localization of the Suppressing Region. To localize the residues involved in the P4110 compensation of G_{438}Q and S_{446}Y, block mutagenesis was performed on pOS4111/site-direct mutants and analyzed for compensation by presence of 130 000-Da protoxin in 24-h cell lysates. After these mutations were constructed and overexpressed, whole cell lysates were analyzed by a SDS–PAGE. Figure 6 shows that pOS4111/G_{438}Q does not possess a 130 000-Da protoxin band in the cell lysates. When block 2 mutations were introduced into pOS4111/G_{438}Q to make pOS4111/G_{438}Q/block 2, a 130 000-Da protoxin band can be seen in lane 3. The lack of the protoxin band in lane 4 suggests that the block 3 mutation offers no compensation for pOS4111/G_{438}Q. No protoxin band is found from 24-h cell lysates of pOS4111/S_{446}Y (lane 5). In the case of the pOS4111/S_{446}Y/block 2 construction, compensation occurred and the protoxin band can be seen (lane 6). In the case of pOS4111/S_{446}Y/block 3, no protoxin

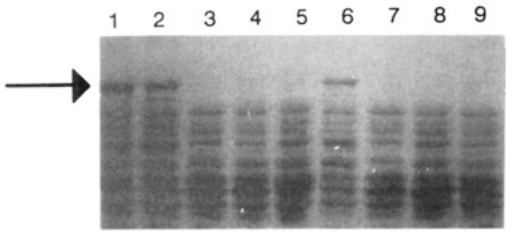

FIGURE 7: Twenty-four-hour whole cell lysates of block mutants. Lane 1, pOS4102; lane 2, pOS4111; lane 3, pOS4111/block 2; lane 4, pOS4111/block 3; lane 5, pOS4111/G_{438}Q; lane 6, pOS4111/G_{438}Q/block 2; lane 7, pOS4111/G_{438}Q/P_{347}Q; lane 8, pOS4111/G_{438}Q/V_{348}Q; lane 9, pOS4111/G_{438}Q/L_{349}R. The arrow indicates the 130 000-Da protoxin band.

Table IV: Ts Values Comparing pOS4110/Site-Direct Mutants and pOS4111/Site-Direct Mutants/Block 2

toxin	Ts[a] mean	toxin	Ts[a] mean
P4110	58 ± 2		
P4110/G_{438}Q	54 ± 2[b]	P4110/S_{446}Y	55 ± 2
P4111/G_{438}Q/block 2	53 ± 2	P4111/S_{446}Y/block 2	52 ± 1

[a] Ts values are in degrees Celsius. [b] Standard deviation in degrees Celsius.

band is seen in lane 7 and thus does not compensate for this mutation.

pOS4111/G_{438}Q/block 2 (Figure 7, lane 6) is shown to possess a 130 000-Da protoxin band. The individual components of block 2 (P_{347}, V_{348}, and L_{349}) were changed by site-directed mutagenesis from CryIAa residues into CryIAc residues as in the block mutagenesis experiment. Whole cell lysates of the constructs pOS4111/G_{438}Q/P_{347}Q, pOS4111/G_{438}Q/V_{348}Q, and pOS4111/G_{438}Q/L_{349}R were analyzed by SDS–PAGE for protoxin accumulation. The results indicate that neither P_{347}Q, V_{348}Q, nor L_{349}R, alone, offers compensation for pOS4111/G_{438}Q. No accumulation of protoxin could be seen in lanes 7, 8, or 9 of Figure 7.

Also of interest in Figure 7 is that pOS4111/block 2 (lane 3) and pOS4111/block 3 (lane 4) exhibit a lack of protoxin accumulation. Lane 2, pOS4111, shows the accumulation of protoxin, but the POS4111/block 2 and POS4111/block 3 mutants demonstrate a loss of the 130 000-Da protoxin accumulation in whole cell lysates.

To determine whether the degree of compensation for P4111/G_{438}Q/block 2 and P4111/S_{446}Y/block 2 was the same as for P4110/G_{438}Q and P4110/S_{446}Y, analysis of the protein stability was performed by the modified thermolysin/temperature protocol. Table IV shows that P4110 possesses a Ts value of 58 °C, but with the site-directed mutants this Ts value has been lowered. P4110/G_{438}Q and P4110/S_{446}Y possess roughly the same reduced Ts value. P4111/G_{438}Q/block 2 does show a slight decrease in Ts value of 1 °C when compared to P4110/G_{438}Q. When comparing P4111/S_{446}Y/block 2 to P4110/S_{446}Y, a Ts value decrease of 3 °C is found for P4111/S_{446}Y/block 2.

DISCUSSION

Chimerical proteins involving an exchange of the *Cla*I–*Sac*I region between *cryIAa* and *cryIAc* demonstrated reduced insecticidal activity to *B. mori* (Ge et al., 1989; Lee et al., 1991), *H. virescens* and *T. ni* (Ge et al., 1991; Schnepf et al., 1990), and *M. sexta* (Schnepf et al., 1990). To determine the significance of this region for *B. mori* and *M. sexta* activity, site-directed mutagenesis was performed on one of the chimeric genes constructed, pOS4111. The mutagenesis was an attempt to restore the *B. mori* activity to P4111. Five residues in the P4111 protein were changed to their P4102 counterparts (Figure 1). We incorporated nonconservative changes in residue side chains in an attempt to affect the greatest change in protein function or structure. The P4111 residues singled out for site-directed mutagenesis were residues with large and/or charged side chains. This region consists of only 22 residues. A comparison of the *Cla*I–*Sac*I region (residues 428–450) between CryIAa and CryIAc toxins can be made by alignment of residues to give the best possible match. This comparison reveals many nonconservative amino acid differences (Figure 1). Of the 22 residues within this region, 13 residue differences are found. These residue differences consist of nonconserved, conserved, and misalignment residues according to Dayhoff et al. (1989).

After completion of the site-directed mutagenesis, the mutant protoxins were bioassayed for *B. mori* and *M. sexta* insecticidal activity. The results indicate that three of the five mutants constructed within this *Cla*I–*Sac*I region (P4111/G_{438}Q, P4111/ΔF_{439}, and P4111/S_{446}Y) showed a reduction in *B. mori* and *M. sexta* insecticidal activity (Tables I and II). The *B. mori* bioassay data for P4111/ΔF_{435} and P4111/R_{436}L showed a decrease in toxicity for both of these site-directed mutants. However, the ranges for P4111 and P4111/ΔF_{435} do overlap, suggesting a slight but not significantly different activity from P4111. P4111/R_{436}L does have a significant decrease in *B. mori* insecticidal activity when compared to P4111.

Schnepf et al. (1990) reported that a nonreciprocal substitution of the *Cla*I–*Sac*I region (identical to P4211) lowered insecticidal activity toward *M. sexta* and concluded that this region is the *M. sexta* specificity determining region. A true *M. sexta* specificity determining region would be expected to increase *M. sexta* insecticidal activity in the reciprocal exchange, which would be P4111 in this case. We performed *M. sexta* bioassays on P4111 and P4211 and observed that P4111 possesses close to a 3-fold reduction when compared to P4102, while P4211 demonstrates at least a 50-fold reduction as compared to P4202 (Table II). Since neither P4111 or P4211 possessed an increase in *M. sexta* activity, we conclude that the *Cla*I–*Sac*I region (residues 428–450) is not the *M. sexta* specificity determining region.

Three of the site-directed mutants, P4111/G_{438}Q, P4111/ΔF_{439}, and P4111/S_{446}Y, possess a greatly reduced insecticidal activity against *M. sexta*. P4111/ΔF_{435} and P4111/R_{436}L possess a slight decrease in activity when compared to P4111. For P4111, P4111/ΔF_{435}, and P4111/R_{436}L, all the ranges overlap in the *M. sexta* bioassay data suggesting a less than significant difference between these toxins.

To determine if the reduction in insecticidal activities is due to alterations in protein structure, methods to ascertain protein stability of the chimeric and mutagenized proteins were utilized. Trypsin-resistant cores were found in P4111/ΔF_{435} and P4111/R_{436}L (Figure 2). In a previous report, midgut protease resistant toxins were generated for P4111 and P4211 (Ge et al., 1991). The other three site-directed mutants, P4111/G_{438}Q, P4111/ΔF_{439}, and P4111/S_{446}Y, were sensitive to *E. coli* intracellular proteases, and the 130 000-Da protoxin band was absent in the whole cell lysates (Figure 3, lanes 6, 7, and 8). Sensitivity to intracellular proteolysis has been demonstrated to correlate with alterations in protein stability (Pakula & Sauer, 1989). A western blot of these three mutants cell lysates demonstrates that minute quantities of the protoxin are present (data not shown).

The P4111 and P4211 toxins show decreases in thermal stability, with P4211 showing the greatest reduction in thermal stability of 6 °C when compared to P4202. P4111 also possess

a significantly different thermal stability from P4102. Differences in protein stability have been correlated with alterations in the protein structure (Alber & Matthews, 1987). The Ts data for P4111, P4111/ΔF_{435}, and P4111/$R_{436}L$ show overlapping standard deviations suggesting that these two site-directed mutations, ΔF_{435} and $R_{436}L$, might alter the protein stability slightly but not to a significant degree. Utilizing the T-test methodology (α = 0.01), the Ts values for P4111, P4111/ΔF_{435}, and P4111/$R_{436}L$ were determined not to be significantly different from each other. We suggest that the large decreases in insecticidal activity of P4111, P4211, and three of the five P4111/site-directed mutants might be due to alterations in the protein structure caused by the mutagenesis of structurally important residues located within residues 428–450 (or the *ClaI–SacI* region) of the Cry proteins.

The radical protein structural alterations that were observed in the mutations $G_{438}Q$, ΔF_{439}, and $S_{446}Y$ could be suppressed when they were individually cloned into pOS4202 (entire *cryIAc* background) or into pOS4110 (nucleotides 996–1287 corresponding to CryIAc residues 332–429). This suggested that the region of the CryIAc protein structure between residues 332 and 428 complemented or suppressed the structural instability of these mutations.

To localize which residues are important in the P4110/$G_{438}Q$ and P4110/$S_{446}Y$ compensation, two blocks of residues were changed by site-directed mutagenesis. These two blocks were chosen by inspection of the CryIAa and CryIAc primary amino acid sequences within the 332 to 428 region. Considering nonconserved residues differences, we constructed mutations consisting of residues 347–349 ($P_{347}Q$, $V_{348}Q$, $L_{349}R$, or block 2) and residues 370–373 and residue 375 ($I_{370}P$, $L_{371}F$, $G_{372}N$, $S_{373}I$, and $P_{375}I$, block 3).

In the case of pOS4111/$G_{438}Q$, block 2 mutation compensates for the alteration in protein structure and thus protoxin can be seen (Figure 6, lane 3). pOS4111/$S_{446}Y$ is also found to be compensated by the same block mutation, block 2 (Figure 6, lane 6). Block 3 exchanges had no compensatory effects for either $G_{438}Q$ or $S_{446}Y$. In order to determine the specific residue in block 2 responsible for this compensation, the individual members of block 2 were changed by site-directed mutagenesis. No compensation in the form of protoxin accumulation was found for pOS4111/$G_{438}Q$/$P_{347}Q$, pOS4111/$G_{438}Q$/$V_{348}Q$, or pOS4111/$G_{438}Q$/$L_{349}R$ (Figure 7, lanes 7, 8, and 9). In summary, the entire block 2 must be changed to compensate for pOS4111/$G_{438}Q$.

Also interesting is the pOS4111/block 2 and pOS4111/block 3 data demonstrating that these block mutations affect the protein structure of the toxin in such a way as to make the protoxin susceptible to intracellular proteases (Figure 7, lanes 3 and 4, respectively). This suggests the block 2 alters the protein structure of the protoxin in such a way as to offer compensation for both $G_{438}Q$ and $S_{446}Y$. Thus, both the initial destabilizing mutations and the compensating block mutations cause destabilization of the protein structure, but together they restore structural stability.

Protein stability can be restored to mutant proteins in an allele-specific manner by the introduction of a compensating substitution or, alternatively, in a global manner by introducting new stabilizing forces. The most common type of second-site suppressor mutations are those that act globally to overcome the original defect by increasing protein stability. Second-site suppressor mutations of the λ Cro repressor protein that increase the thermodynamic stability of unstable mutant proteins have been shown to introduce new stabilizing forces that act globally (Pakula & Sauer, 1989; Hecht & Sauer, 1985).

To determine if block 2 mutagenesis has the same degree of compensation as the P4110 construct, all four of the toxins' protein stability were measured by the thermolysin/temperature protocol. The Ts values of P4111/$G_{438}Q$/block 2 and P4111/$S_{446}Y$/block 2 are slightly lower than the Ts values for the P4110/$G_{438}Q$ and P4110/$S_{446}Y$ (Table IV), but no significant difference could be found between the four Ts values as determined by the T-test method (α = 0.01). This suggests that the major factors involved in the P4110 compensation of $G_{438}Q$ and $S_{446}Y$ are the three residues involved in the block 2 mutation.

A *cryIAc* gene was cloned from *B. thuringiensis* subspecies *kenyae* that gene encodes a CryIAc protein with slightly reduced insecticidal activity when compared to *B. thuringiensis* subspecies *kurstaki* CryIAc. Upon amino acid comparison of *B. thuringiensis* subspecies *kenyae* CryIAc and *B. thuringiensis* subspecies *kurstaki* CryIAc, seven amino acid differences can be found. Some of the differences in the amino acids between the two proteins tend to be conservative substitutions of hydrophobic residues. Three residue differences of relevance to this work are $F_{336}L$, $S_{440}F$, and ΔN_{442}. The last two differences, $S_{440}F$ and ΔN_{442}, cause a slight hydrophilic peak in an otherwise hydrophobic region. These substitutions, as theorized by Von Tersch et al. (1991), may be functionally or structurally complemented by reverse substitutions at other residues. $F_{336}L$ is located between block 2 and block 3, while $S_{440}F$ and ΔN_{442}, are found within the *ClaI–SacI* region. These amino acid differences between *B. thuringiensis* subspecies *kenyae* CrylAc and *B. thuringiensis* subspecies *kurstaki* CryIAc closely resemble the structural compensation seen by the block mutants and the *ClaI–SacI* mutants found in this work.

Recently, the CryIIIA three-dimensional protein structure has been determined (Li et al., 1991). The five highly conserved amino acid tracts found in all Cry proteins (Höfte & Whiteley, 1987) were determined to be located as internal structures for the CryIIIA protein. On the basis of this observation, Li et al. (1991) proposed that all Cry proteins would adopt similar if not the same three-dimensional structure. On the basis of our best residue and secondary protein structure alignment between CryIAa, CryIAc, and CryIIIA toxins, the structural assignments for the mutants are as follows: block 2 (β-sheet 5), block 3 (β-loop 2), ΔF_{435} and $R_{436}L$ (β-sheet 10), and $G_{438}Q$, ΔF_{439}, and $S_{446}Y$ (β-loop 3). The exact positions for these mutations, whether internal or external, are unknown at this time because the CryIIIA corrdinates have not been published. Also, it is unclear whether the CryIIIA secondary structures will correlate to CryIA secondary protein structures. For these reasons, we do not believe we can propose locations for the mutations ΔF_{435}, $R_{436}L$, $G_{438}Q$, ΔF_{439}, $S_{446}Y$, block 2, and block 3.

In conclusion, we theorize we have located three regions that are of structural importance to the CryIA toxins. We suggest that the *ClaI–SacI* region (residues 428–450), block 2 (residues 347–349), and block 3 (residues 370–373 and residue 375) interact in a manner that can stabilize the protein structure.

ACKNOWLEDGMENT

We thank Ross Milne and the FPMI, Sault Ste. Marie, Ontario, Canada, and Michael Jackson of the USDA, Oxford, NC, for generously supplying us with the insect eggs used in this study.

REFERENCES

Alber, T., & Matthews, B. W. (1987) in *Protein Engineering* (Oxender, D. L., & Fox, C. F., Eds.) pp 280–297, Alan Liss, Inc., New York.

Andrew, R. E., Faust, R. M., Wabiko, H., Raymond, K. C., & Bulla, L. A. (1987) *CRC Crit. Rev. Biotechnol. 6*, 163–232.

Chestukhina, G. G., Kostina, L. I., Mikhailova, A. L., Tyurin, S. A., Klepikova, F. S., & Strepanov, V. M. (1982) *Arch. Microbiol. 132*, 159–162.

Dayhoff, M. O., Schwartz, R. M., & Orcutt, B. C. (1987) *Atlas Protein Seq. Struct. 5*, 435–352.

Ge, A. Z., Shivarova, N. I., & Dean, D. H. (1989) *Proc. Natl. Acad. Sci. U.S.A. 86*, 4037–4041.

Ge, A. Z., Rivers, D., Milne, R., & Dean, D. H. (1991) *J. Biol. Chem. 66*, 17954–17958.

Gent, M. E., Gartner, S., Gronenborn, A. M., Sandulache, R., & Clore, G. M. (1987) *Protein Eng. 1*, 201–203.

Harvey, W. R., & Wolfersberger, M. G. (1979) *J. Exp. Biol. 53*, 293–304.

Hecht, M. H., & Sauer, R. T. (1985) *J. Mol. Biol. 186*, 53–63.

Hofmann, C., Lüthy, P., Hutter, R., & Pliska, V. (1988) *Eur. J. Biochem. 173*, 85–91.

Höfte, H., & Whiteley, H. R. (1989) *Microbiol. Rev. 53*, 242–255.

Huber, H. E., Lüthy, P., Edersold, H. R., & Cordier, J.-L. (1981) *Arch. Microbiol. 129*, 14–18.

Kunkel, T. A. (1985) *Proc. Natl. Acad. Sci. U.S.A. 82*, 488–492.

Laemmli, U. K. (1970) *Nature 227*, 680–685.

Lee, M. K., Milne, R. E., Ge, A. Z., & Dean, D. H. (1992) *J. Biol. Chem. 267*, 3115–3121.

Li, J., Carrol, J., & Ellar, D. J. (1991) *Nature 353*, 815–821.

McLinden, J. H., Sabourin, J. R., Clark, B. D., Gensler, D. R., Workman, W. E., & Dean, D. H. (1985) *Appl. Environ. Microbiol. 50*, 623–628.

Milne, R., Ge, A. Z., Rivers, D., & Dean, D. H. (1990) in *Analytical Chemistry of Bacillus thuringiensis* (Hickle, L., & Fitch, B., Eds.) pp 22–35, American Chemical Society, Washington, D.C.

Nakamura, K., Oshie, K., Shimizu, M., Takada, Y., Oeda, K., & Ohkawa, H. (1990) *Agric. Biol. Chem. 54*, 715–724.

Paukla, A. A., & Sauer, R. T. (1989) *Proteins: Struct., Funct., Genet. 5*, 202–210.

Raymond, M. (1985) *Cah. ORSTOM, Ser. Entomol. Med. Parasitol. 22*, 117–121.

Schnepf, H. E., Tomaczak, K., Ortega, J. P., & Whiteley, H. R. (1990) *J. Biol. Chem. 265*, 20923–20930.

Widner, W. R., & Whiteley, H. R. (1990) *J. Bacteriol. 172*, 2826–2832.

Vieira, J., & Messing, J. (1982) *Methods Enzymol. 153*, 3–11.

Von Tersch, M. A., Robbins, H. L., Jany, C. S., & Johnson, T. B. (1991) *Appl. Environ. Microbiol. 57*, 349–358.